Effects of Magnesium(II) Ion on Hydride-transfer Reactions from an NADH Model Compound to *p*-Benzoquinone Derivatives. The Quantitative Evaluation based on the Reaction Mechanism

Shunichi Fukuzumi, Nobuaki Nishizawa, and Toshio Tanaka *
Department of Applied Chemistry, Faculty of Engineering, Osaka University, Suita, Osaka 565, Japan

The effects of Mg^{2+} ion on hydride-transfer reactions from an NADH model compound, 1-benzyl-1,4-dihydronicotinamide (BNAH), to a series of *p*-benzoquinone derivatives (Q) as well as on the redox potentials of BNAH and Q in acetonitrile have been examined. The Mg^{2+} ion shows both accelerating and retarding effects on the hydride-transfer reactions depending on the *p*-benzoquinone derivative and the Mg^{2+} concentration. Such dual effects of the Mg^{2+} ion have been well correlated with the change of the redox potentials of BNAH and Q in the presence of Mg^{2+} ion since it has been found that there is a simple correlation between the logarithm of the rate constant and the difference of the redox potentials between BNAH and Q in the absence and presence of Mg^{2+} ion. It is shown that a proposed reaction mechanism involving electron transfer from BNAH to Q followed by proton transfer from $BNAH^{+\bullet}$ to $Q^{-\bullet}$ in the rate-determining step of the hydride-equivalent transfer provides a quantitative evaluation of the single and unified correlation between the logarithm of the rate constant and the difference between the redox potentials of BNAH and Q in the absence and presence of Mg^{2+} ion. The effect of Mg^{2+} ion on the primary kinetic isotope effects on hydride transfer from BNAH to Q is also shown to be consistent with the proposed reaction mechanism. Moreover, a ternary complex involving BNAH, Mg^{2+} ion, and Q as a reaction intermediate prior to electron transfer from BNAH to Q has been detected for the first time.

The mechanisms of hydride-transfer reactions from NADH and its model compounds to substrates have been the subject of considerable controversy, largely revolving around the depiction of the transition states, whether there may be only one transition state (*i.e.* a hydride transfer occurs in a single step)[1-5] or multiple transition states (*i.e.* a hydride-equivalent transfer consists of overall transfer of two electrons and a proton in a e^{-}–H^{+}–e^{-} sequence).[6-9] However, such mechanistic distinction (single step *versus* multistep) seems to be actually dubious and possibly even meaningless unless either mechanism provides a more quantitative description of the activation barriers of the hydride-equivalent transfer reactions than does the other. Indeed, there is surprisingly little quantitative interpretation of the activation barrier based on either reaction mechanism despite abundant literature on this subject.[1-9] Recently, Kreevoy and his co-workers[10] have demonstrated that rate constants of hydride-transfer reactions between the reduced and oxidized forms of various substituted pyridinium ions or 5-deazaflavin can be predicted from the equilibrium constants of the hydride transfer by applying the Marcus theory of atom transfer,[11] based on a single-step hydride-transfer mechanism. However, their data have not permitted a complete test of the predicted variation of the Brönsted slope or the primary kinetic isotope effects with the equilibrium constants.

In previous work,[12] we have presented an alternative approach to the study of hydride-transfer reactions from an NADH model compound, 1-benzyl-1,4-dihydronicotinamide (BNAH), to a series of *p*-benzoquinone derivatives in acetonitrile (MeCN), succeeding in simulating not only the rate constants k but also the primary kinetic isotope effects k_H/k_D as a function of the redox potentials of BNAH and Q based on a reaction mechanism of equations (1) and (2). In this mechanism, a hydride-equivalent transfer from BNAH to a *p*-benzoquinone derivative (Q) occurs in an electron–proton–electron sequence through the charge-transfer (CT) complex formed between BNAH and Q. The existence of the CT complex as a reaction intermediate has been demonstrated by its isolation and the comparison of the transient CT spectrum observed during the reaction with that of the isolated complex. The distinction between the single-step and multistep mechanism is considered to depend on the lifetime of the radical ion pair $[BNAH^{+\bullet}Q^{-\bullet}]$ in equations (1) and (2).[12]

$$BNAH + Q \overset{K_{CT}}{\rightleftharpoons} [BNAH\ Q] \underset{k_{-1}}{\overset{k_1}{\rightleftharpoons}} [BNAH^{+\bullet}\ Q^{-\bullet}] \quad (1)$$

$$[BNAH^{+\bullet}\ Q^{-\bullet}] \xrightarrow{k_H} [BNA^{\bullet}\ QH^{\bullet}] \xrightarrow{fast} BNA^{+} + QH^{-} \quad (2)$$

On the other hand, the effects of metal ions such as Mg^{2+} and Zn^{2+} ions on hydride-transfer reactions from NADH model compounds to substrates have also attracted considerable interest in relation to the role of metal ions in the redox reactions of nicotinamide coenzymes.[13] In particular, Mg^{2+} ion is known to accelerate or retard the hydride-transfer reactions depending on the substrates and the Mg^{2+} concentration.[14-17] Any reaction mechanisms for hydride-transfer reactions from NADH model compounds to substrates, if the mechanistic description is to have any general value, must also resolve the difficult problem of the reason for such dual effects of metal ions, although no satisfactory explanation for the effects of metal ions on the hydride-transfer reactions has so far been given quantitatively based on either the single-step or multistep mechanism.

In the present study, we show that equations (1) and (2) can also provide a quantitative evaluation of the effects of Mg^{2+} ion on the hydride-transfer reactions from BNAH to Q in MeCN. Since both the rate constants and the primary kinetic isotope effects in the absence of Mg^{2+} ion have been simulated as a function of the redox potentials of BNAH and Q,[12] we first examine the effects of Mg^{2+} ion on the rate constants and the primary kinetic isotope effects for the hydride-transfer reactions from BNAH to Q and then determine the redox potentials of BNAH and Q in the presence of Mg^{2+} ion in MeCN, which offers an excellent opportunity to develop a quantitative evaluation of the effects of Mg^{2+} ion based on the reaction mechanism [equations (1) and (2)]. The detection of an

intermediate ternary complex involving BNAH, Mg^{2+} ion, and Q in the hydride-transfer reactions is also reported for the first time.[18]

Experimental

Materials.—1-Benzyl-1,4-dihydronicotinamide (BNAH) and [4-^{2}H]-1-benzyl-1,4-dihydronicotinamide were prepared by the literature method.[19] [4,4-$^2H_2$]-1-benzyl-1,4-dihydronicotinamide was prepared from [4-^{2}H]BNAH by three cycles of oxidation with *p*-chloranil in dimethylformamide and reduction with dithionite in deuterium oxide.[20] The deuterium content of [4,4-$^2H_2$]BNAH was determined to be 96% by ^{1}H n.m.r. measurements on a JEOL JNM-PS-100 spectrometer (100 MHz). Most *p*-benzoquinone derivatives (*p*-chloranil, *p*-bromanil, 2,3-dichloro-5,6-dicyano-*p*-benzoquinone, 2,6-dichloro-*p*-benzoquinone, 2,5-dichloro-*p*-benzoquinone, *p*-benzoquinone, methyl-*p*-benzoquinone, 2,6-dimethyl-*p*-benzoquinone, and tetramethyl-*p*-benzoquinone) were obtained commercially and purified by standard methods.[21] Chloro-*p*-benzoquinone, 2,3-dicyano-*p*-benzoquinone, and trimethyl-*p*-benzoquinone were prepared from the corresponding hydroquinones according to the literature.[22] The radical anion salt of *p*-chloranil (Na^+*p*-chloranil$^{-\bullet}$) was prepared by the one-electron reduction of *p*-chloranil with NaI in MeCN solution.[23] Anhydrous magnesium perchlorate was obtained from Wako Pure Chemicals. Acetonitrile used as a solvent was purified and dried by the standard procedure[21] and stored over calcium hydride under nitrogen.

Kinetic Measurements.—Kinetic measurements were carried out by using a Union RA-103 stopped-flow spectrophotometer and a Union SM-401 spectrophotometer for hydride-transfer reactions from BNAH to Q in the presence of Mg^{2+} ion in MeCN at 298 K under deaerated conditions with half-lives < 10 s and > 100 s, respectively. Reaction rates were followed by the decay of the absorption band due to BNAH ($\lambda_{max.}$ 363 nm in the presence of Mg^{2+} ion in MeCN) under pseudo-first-order conditions using >10-fold excess of Q. Pseudo-first-order rate constants were determined by least-squares curve fitting using a Union system 77 microcomputer.

The primary kinetic isotope effects were determined from pairs of experiments carried out using portions of freshly prepared MeCN solutions containing a large excess of Q to which BNAH or [4,4-$^2H_2$]BNAH was added to start the reaction.

Cyclic Voltammetry.—Redox potentials of BNAH and Q in the presence of Mg^{2+} ion in MeCN were determined by cyclic voltammetry (CV) measurements at various sweep rates (20—1 000 mV s^{-1}), based on the method described in detail elsewhere.[24,25] The CV measurements were performed on a Hokuto Denko model HA-301 potentiostat–galvanostat at 298 K using a platinum microelectrode and a standard NaCl calomel reference electrode (s.c.e.) under deaerated conditions. The platinum microelectrode was routinely cleaned by soaking it in concentrated nitric acid, followed by repeated rinsing with water and acetone, and drying at 353 K prior to use. The anodic and cathodic peak potentials of BNAH and Q, respectively, of the first scan were reproducible to within ± 20 mV at a constant sweep rate although the peak currents decreased on repeating the scan.

Results

Kinetics.—It has previously been reported that the hydride transfer from BNAH to *p*-benzoquinone derivatives Q [equation (3)] occurs in MeCN followed by a subsequent fast reaction of QH^- with Q to form $Q^{-\bullet}$ and QH_2 [equation (4)].[12] When $Mg(ClO_4)_2$ was added to the BNAH–Q system, only the hydride-transfer reaction [equation (3)] occurred and the radical anion $Q^{-\bullet}$ was not formed as confirmed from the electronic spectrum.[12]

$$BNAH + Q \xrightarrow{k} BNA^+ + QH^- \quad (3)$$

$$2QH^- + Q \xrightarrow{fast} 2Q^{-\bullet} + QH_2 \quad (4)$$

Rates of the hydride-transfer reactions from BNAH to Q in the presence of Mg^{2+} ion in MeCN were followed by the decay of the BNAH concentration determined from the absorbance at 363 nm, which can be expressed by the second-order kinetics [equation (5)]. The rate constants k were determined under

$$-d[BNAH]/dt = k[BNAH][Q] \quad (5)$$

pseudo-first-order conditions in the presence of a large excess of Q. A typical example of the dependence of k on the Mg^{2+} concentration is shown in Figure 1, where the k value for the hydride-transfer reaction from BNAH to 2,6-dichloro-*p*-benzoquinone in MeCN at 298 K decreases sharply with increasing Mg^{2+} concentration at low concentrations ($\ll 0.10$ mol dm^{-3}), while the k value increases for high concentrations (>0.10 mol dm^{-3}). Thus, the Mg^{2+} ion shows both retarding and accelerating effects on the hydride-transfer reaction depending on the Mg^{2+} concentration. Second-order rate constants k for hydride-transfer reactions from BNAH to a series of *p*-benzoquinone derivatives in the presence of 1.0×10^{-2}, 1.0×10^{-1}, and 1.6 mol dm^{-3} Mg^{2+} ion in MeCN at 298 K are listed in Table 1, together with those in the absence of Mg^{2+} ion reported previously.[12] The rate constants were replicated 4—20 times, giving average deviations from the mean values in Table 1 within $\pm 5\%$.

Effects of Mg^{2+} ion on the primary kinetic isotope effects k_H/k_D have also been determined from the ratio of the rate constants k of BNAH to that of [4,4-$^2H_2$]BNAH in the presence of 1.0×10^{-2}, 1.0×10^{-1}, and 1.6 mol dm^{-3} Mg^{2+} ion in MeCN at 298 K, assuming that the secondary kinetic isotope effect is unity, which has been confirmed in the absence of Mg^{2+} ion.[12] The k_H/k_D values were determined from pairs of experiments carried out under identical conditions so that the experimental error in k_H/k_D is $< \pm 5\%$ (see Experimental section). The results are listed in Table 2, together with those in the absence of Mg^{2+} ion.[12]

Detection of a Ternary Complex as a Reaction Intermediate.—Mixing of high concentrations of BNAH (4.29×10^{-2} mol dm^{-3}) with 2,6-dichloro-*p*-benzoquinone (9.68×10^{-2} mol dm^{-3}) in the absence of Mg^{2+} ion in MeCN by using a stopped-flow spectrophotometer displays an instant rise of a charge-transfer (CT) band of the BNAH–2,6-dichloro-*p*-benzoquinone complex in the long-wavelength region as shown by the open circles in Figure 2. When Mg^{2+} ion is added to the BNAH–2,6-dichloro-*p*-benzoquinone system, the transient CT band observed in the absence of Mg^{2+} ion ($\lambda_{max.}$ 680 nm; $h\nu_{CT}$ 1.82 eV) is significantly blue-shifted in the presence of 0.10 mol dm^{-3} Mg^{2+} ion ($\lambda_{max.}$ 600 nm; $h\nu_{CT}$ 2.07 eV) as shown by the filled circles in Figure 2. A similar blue-shift of the CT band of the BNAH–*p*-chloranil complex is observed in the presence of 0.10 mol dm^{-3} Mg^{2+} ion as shown by triangles in Figure 2. Since the Mg^{2+} ion is known to form a 1 : 1 complex with BNAH in MeCN with the formation constant 1.2×10^4 mol^{-1} dm^3 [equation (6)],[17] the change of the transient CT band by the addition of Mg^{2+} ion (Figure 2) may be explained by the formation

$$BNAH + Mg^{2+} \underset{}{\overset{K}{\rightleftharpoons}} [BNAH\ Mg^{2+}] \quad (6)$$

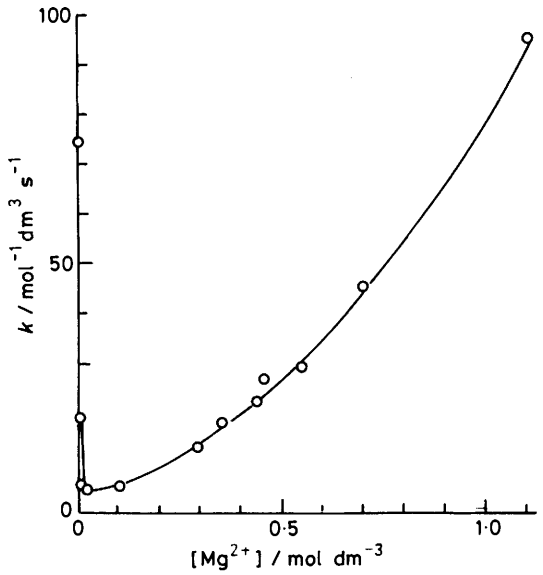

Figure 1. Variation of the rate constant k for the hydride-transfer reaction from BNAH [(1.23—2.18) × 10^{-4} mol dm^{-3}] to 2,6-dichloro-*p*-benzoquinone [(1.32—4.65) × 10^{-3} mol dm^{-3}] with the Mg^{2+} concentration in MeCN at 298 K

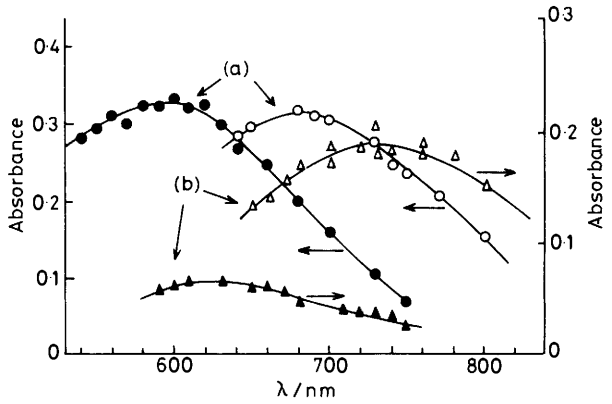

Figure 2. Transient charge-transfer spectra obtained by plotting the initial absorbances of the kinetic curves against the wavelengths (a) in the reaction of BNAH (2.22 × 10^{-2} mol dm^{-3}) with 2,6-dichloro-*p*-benzoquinone (1.45 × 10^{-2} mol dm^{-3}) in the absence of Mg^{2+} ion (○) and that of BNAH (4.29 × 10^{-2} mol dm^{-3}) with 2,6-dichloro-*p*-benzoquinone (9.68 × 10^{-2} mol dm^{-3}) in the presence of Mg^{2+} ion (1.0 × 10^{-1} mol dm^{-3}) (●); (b) in the reaction of BNAH (7.35 × 10^{-2} mol dm^{-3}) with *p*-chloranil (1.01 × 10^{-2} mol dm^{-3}) in the absence of Mg^{2+} ion (△) and that of BNAH (9.68 × 10^{-2} mol dm^{-3}) with *p*-chloranil (1.03 × 10^{-2} mol dm^{-3}) in the presence of Mg^{2+} ion (1.0 × 10^{-1} mol dm^{-3}) (▲) in MeCN at 298 K

of a ternary complex involving BNAH, Mg^{2+} ion, and a *p*-benzoquinone derivative Q as a reaction intermediate for the hydride-transfer reaction from BNAH to Q [equation (7)].

$$\text{BNAH} + Mg^{2+} + Q \rightleftharpoons [\text{BNAH } Mg^{2+}\ Q] \longrightarrow \text{BNA}^+ + Mg^{2+} + QH^- \quad (7)$$

Indeed, the decay of the CT band in the presence of Mg^{2+} ion due to [BNAH Mg^{2+} Q] coincided with the decay of the absorption band due to BNAH. The $\lambda_{max.}$ values for ternary complexes of other *p*-benzoquinone derivatives such as *p*-benzoquinone and methyl-substituted *p*-benzoquinones having more negative reduction potentials than 2,6-dichloro-*p*-benzoquinone have not been observed distinctly because of overlap of the CT bands with the absorption bands due to the *p*-benzoquinone derivatives.

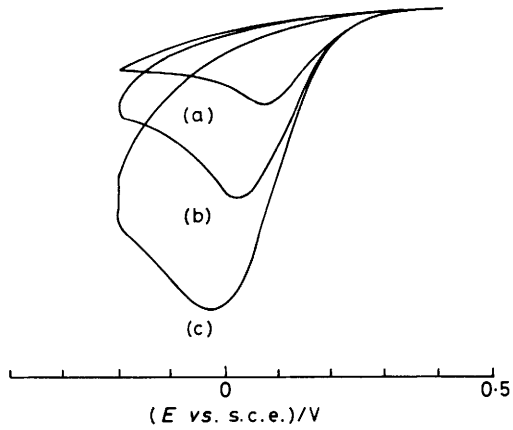

Figure 3. Cyclic voltammograms of 2,5-dichloro-*p*-benzoquinone (1.0 × 10^{-2} mol dm^{-3}) in MeCN containing $Mg(ClO_4)_2$ (1.6 mol dm^{-3}) at various sweep rates: (a) 10, (b) 100, (c) 333 mV s^{-1}

Determination of Redox Potentials of Q and BNAH in the Presence of Mg^{2+} *Ion.*—The electrochemical reduction of *p*-benzoquinone derivatives Q in MeCN are reversible and the half-wave potentials are good estimates of the standard redox potentials of the couple Q–$Q^{-\bullet}$.[26] When Mg^{2+} ion is added to a MeCN solution of Q, the electrochemical reduction occurs irreversibly as shown in Figure 3, where the cyclic voltammograms of 2,5-dichloro-*p*-benzoquinone in MeCN containing 1.6 mol dm^{-3} $Mg(ClO_4)_2$ at different sweep rates are illustrated as typical examples. The cyclic voltammogram in Figure 3 is characterized by a cathodic wave showing a well defined current maximum but no coupled anodic wave on the reverse scan even at sweep rates up to 1 000 mV s^{-1}. Such an irreversible reduction of Q indicates that the follow-up chemical reaction in the presence of Mg^{2+} ion [equation (8)] is fast on the

$$2Q^{-\bullet} + Mg^{2+} \longrightarrow Q + [Q^{2-}\ Mg^{2+}] \quad (8)$$

time-scale of the CV measurements. Indeed, upon mixing a MeCN solution of the radical anion of *p*-chloranil prepared independently (see Experimental section) with Mg^{2+} ion, the disproportionation reaction of $Q^{-\bullet}$ occurs instantly and the stoicheiometry [equation (8)] has been confirmed by the disappearance of the absorption band due to the radical anion of *p*-chloranil ($\lambda_{max.}$ 450 nm, ε 9.00 × 10^4 mol^{-1} dm^2) by the addition of Mg^{2+} ion.

Figure 3 also reveals the negative shift of the reduction peak potential of Q (E_{red}^{p}) as well as a peak broadening on increasing the sweep rate. The width of the cathodic wave ($E_{red}^{p/2} - E_{red}^{p}$) in such an irreversible system is known to depend on the transfer coefficient β according to equation (9),[24,25] where F is the Faraday constant and the other

$$E_{red}^{p/2} - E_{red}^{p} = 1.857\ RT/\beta F \quad (9)$$

notations are conventional. Then, the transfer coefficient β defined by the tangent of the Gibbs energy relationship of electron transfer, *i.e.* $\partial\Delta G^{\ddagger}/\partial\Delta G_{et}^{0}$, at the reduction peak potential E_{red}^{p} can be obtained from the width of the cathodic wave $E_{red}^{p/2} - E_{red}^{p}$ by using equation (9). On the other hand, the Gibbs energy relationship of electron transfer is given by Marcus[27] as shown by equation (10), where $\Delta G_0^{\ddagger}$ is the

$$\Delta G^{\ddagger} = \Delta G_0^{\ddagger}[1 + (\Delta G_{et}^{0}/4\Delta G_0^{\ddagger})]^2 \quad (10)$$

Table 1. Rate constants k for hydride-transfer reactions from BNAH to *p*-benzoquinone derivatives in the absence and presence of Mg^{2+} ion in MeCN at 298 K

Entry	*p*-Benzoquinone derivative	k (mol^{-1} dm^3 s^{-1})[a] at the Mg^{2+} concentration (mol dm^{-3}) of			
		0[b]	1.0×10^{-2}[c]	1.0×10^{-1}[c]	1.6[c]
1	2,3-Dichloro-5,6-dicyano-*p*-benzoquinone	8.4×10^6	2.0×10^4	1.6×10^4	2.0×10^4
2	2,3-Dicyano-*p*-benzoquinone	7.2×10^5	4.6×10^4	2.8×10^4	6.0×10^4
3	*p*-Chloranil	1.0×10^3	4.0×10	1.8×10	5.6×10
4	*p*-Bromanil	7.3×10^2	6.0×10	2.4×10	6.1×10
5	2,6-Dichloro-*p*-benzoquinone	7.5×10	4.5	5.1	1.3×10^2
6	2,5-Dichloro-*p*-benzoquinone	5.0×10	2.9	3.0	9.6×10
7	Chloro-*p*-benzoquinone	7.6	5.9×10^{-1}	1.0	5.3×10
8	*p*-Benzoquinone	1.3×10^{-2}	8.0×10^{-2}	2.7×10^{-1}	1.9×10
9	Methyl-*p*-benzoquinone	2.3×10^{-3}	1.4×10^{-2}	4.4×10^{-2}	3.0
10	2,6-Dimethyl-*p*-benzoquinone	8.4×10^{-5}	9.9×10^{-4}	3.9×10^{-3}	1.7×10^{-1}
11	Trimethyl-*p*-benzoquinone	1.3×10^{-5}	2.1×10^{-4}		4.0×10^{-2}

[a] Determined with accuracy ±5%. [b] Ref. 12. [c] This study.

Table 2. Primary kinetic isotope effects k_H/k_D for hydride-transfer reactions from BNAH to *p*-benzoquinone derivatives in the absence and presence of Mg^{2+} ion in MeCN at 298 K

Entry[b]	k_H/k_D[a] at the Mg^{2+} concentration (mol dm^{-3}) of			
	0[c]	1.0×10^{-2}[d]	1.0×10^{-1}[d]	1.6[d]
1	1.5	2.0	1.9	2.7
2	2.6	4.3	3.7	2.6
3	5.3	5.9	5.8	4.4
4	5.2	5.8	6.1	4.1
5	5.6	5.8	4.3	2.1
6	5.5	6.3	4.6	2.5
7	6.1	5.4	3.5	1.9
8	6.2	5.4	4.3	2.8
9	5.9	5.2	4.1	3.4
10	5.6	4.6	3.6	5.0
11	5.6	4.2		6.1

[a] The experimental error is within ±5%. [b] Numbers refer to *p*-benzoquinone derivatives in Table 1. [c] Ref. 12. [d] This study.

activation Gibbs energy when $\Delta G_{et}^0 = 0$. Thus, the transfer coefficient β is expressed as a function of ΔG_{et}^0 [$= F(E - E_{red}^0)$] by differentiating equation (10) with respect to ΔG_{et}^0 as shown by equation (11), from which is derived a relation

$$\beta = 1/2 + \Delta G_{et}^0/8\Delta G_0^{\ddagger} \quad (11)$$

between the reduction peak potential E_{red}^P and the reduction potential E_{red}^0 which is equal to the standard redox potential of Q [equation (12)] when $\Delta G_{et}^0 = F(E_{red}^P - E_{red}^0)$. According to equation (12), the reduction potential E_{red}^0 can be evaluated

$$E_{red}^P = E_{red}^0 - 4(1 - 2\beta)\Delta G_0^{\ddagger}/F \quad (12)$$

from the intercept of the linear correlation between E_{red}^P and $4(1 - 2\beta)$ in which the β value is obtained from the cyclic voltammogram by using equation (9). Typical examples of the plots of E_{red}^P *versus* $4(1 - 2\beta)$ for *p*-benzoquinone derivatives in the presence of 0.10 and 1.6 mol dm^{-3} Mg^{2+} ion are shown in Figure 4. Similarly, the oxidation potentials E_{ox}^0 of BNAH in the presence of 0.10 and 1.6 mol dm^{-3} Mg^{2+} ion have been determined based on equation (13), which is derived from equation (11) when $\Delta G_{et}^0 = F(E_{ox}^0 - E_{ox}^P)$. The reduction

$$E_{ox}^P = E_{ox}^0 + 4(1 - 2\beta)\Delta G_0^{\ddagger}/F \quad (13)$$

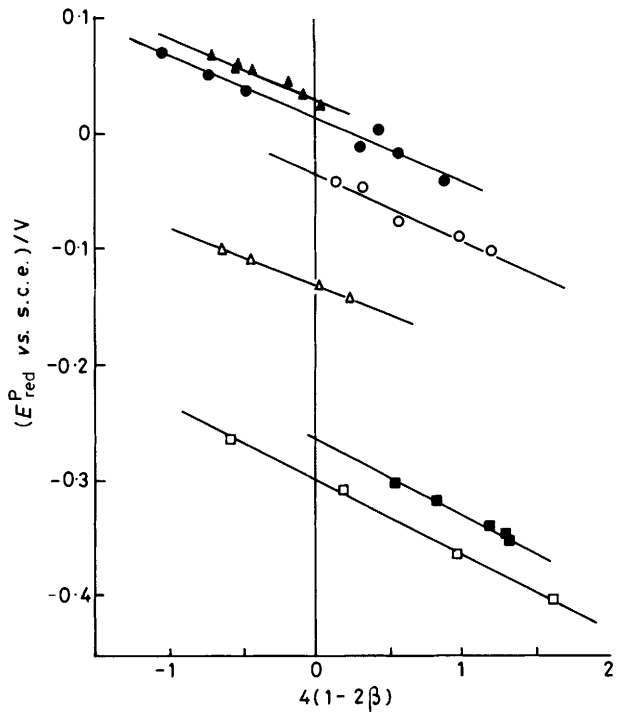

Figure 4. Reduction-peak potentials E_{red}^P (*versus* s.c.e.) of *p*-benzoquinone derivatives (1.0×10^{-2} mol dm^{-3}) in the presence of Mg^{2+} ion in MeCN at 298 K plotted as a function of transfer coefficient β, *i.e.* $4(1 - 2\beta)$, based on the Marcus Gibbs energy relationship, see equation (12); *p*-chloranil in the presence of 1.6 mol dm^{-3} Mg^{2+} ion (▲), 2,5-dichloro-*p*-benzoquinone in the presence of 1.6 mol dm^{-3} Mg^{2+} ion (●), 2,5-dichloro-*p*-benzoquinone in the presence of 0.10 mol dm^{-3} Mg^{2+} ion (○), chloro-*p*-benzoquinone in the presence of 0.10 mol dm^{-3} Mg^{2+} ion (△), trimethyl-*p*-benzoquinone in the presence of 1.6 mol dm^{-3} Mg^{2+} ion (■), 2,6-dimethyl-*p*-benzoquinone in the presence of 0.10 mol dm^{-3} Mg^{2+} ion (□)

potentials of *p*-benzoquinone derivatives, E_{red}^{0*}, and the oxidation potentials of BNAH, E_{ox}^{0*}, in the presence of 0.10 and 1.6 mol dm^{-3} Mg^{2+} ion (the asterisk identifies the value in the presence of Mg^{2+} ion) are listed in Table 3 together with those in the absence of Mg^{2+} ion. It is interesting to note that the reduction potentials of *p*-benzoquinone derivatives having relatively high reduction potentials in the absence of Mg^{2+} ion

Table 3. Redox potentials (*versus* s.c.e.) of *p*-benzoquinone derivatives and BNAH in the absence and presence of Mg^{2+} ion[a]

p-Benzoquinone derivative[b]	Redox potentials at the Mg^{2+} concentration (mol dm^{-3}) of 0[c] E_{red}^0/V	1.0×10^{-1}[d] E_{red}^{0*}[e]/V	1.6[d] E_{red}^{*}[e]/V
1	0.51	0.51	0.51
2	0.28	0.25	0.31
3	0.01	0.03	0.03
4	0.00	−0.04	0.00
5	−0.18	−0.04	0.03
6	−0.18	−0.04	0.01
7	−0.34	−0.13	−0.03
8	−0.50	−0.18	−0.01
9	−0.58	−0.32	−0.10
10	−0.67	−0.30	−0.28
11	−0.75	−0.40	−0.27
	E_{ox}^0/V	E_{ox}^{0*}[e]/V	E_{ox}^{0*}[e]/V
BNAH	0.57	0.80	0.75

[a] Determined with accuracy ±0.03 V. [b] Numbers refer to *p*-benzoquinone derivatives in Table 1. [c] Ref. 12. [d] This study. [e] Asterisk identifies the redox potential in the presence of Mg^{2+} ion.

($E_{red}^0 \geqq 0$ V) are approximately invariant in the presence of 0.10 and 1.6 mol dm^{-3} Mg^{2+} ion, while those having relatively low reduction potentials ($E_{red}^0 \geqq -0.18$ V) are shifted in the positive direction on increasing the Mg^{2+} concentration (Table 3). Such a positive shift of the redox potential is also observed for BNAH as shown in the last row of Table 3, where the oxidation potential of BNAH is shifted in the positive direction (*ca.* +0.2 V) in the presence of 0.10 mol dm^{-3} Mg^{2+} ion, but shows essentially no further positive shift in the presence of much more concentrated Mg^{2+} ion (1.6 mol dm^{-3}).

Discussion

Effects of Mg^{2+} *Ion on Gibbs Energy Relationship for Hydride Transfer from BNAH to Q.*—In Figure 5, the logarithms of rate constants in Table 1 are plotted against the difference between the redox potentials of BNAH and Q in the absence of Mg^{2+} ion in MeCN, $E_{ox}^0 - E_{red}^0$, which is related to the standard Gibbs energy change of electron transfer from BNAH to Q (ΔG_{et}^0) by equation (14). The log *k* value in the absence of Mg^{2+}

$$\Delta G_{et}^0 = F(E_{ox}^0 - E_{red}^0) \quad (14)$$

ion shows a smooth but somehow curved correlation with the $\Delta G_{et}^0/F$ value. On the other hand, the addition of Mg^{2+} ion to the BNAH–Q system results in both the increase and decrease of the log *k* values for *p*-benzoquinone derivatives having lower reduction potentials ($E_{red}^0 < -0.18$ V) and higher reduction potentials ($E_{red}^0 > 0$ V) in Table 3, respectively (Figure 5). Thus, the Mg^{2+} ion shows both accelerating and retarding effects depending on the electron-acceptor ability of *p*-benzoquinone derivatives. Moreover, the accelerating effect of Mg^{2+} ion is enhanced upon increasing the Mg^{2+} concentration from 0.10 to 1.6 mol dm^{-3}, while the retarding effect of Mg^{2+} ion is almost unchanged on increasing the Mg^{2+} concentration (Figure 5). In the following discussion, we show how the reaction mechanism [equations (1) and (2)] can resolve the difficult problem of the complex effects of Mg^{2+} ion on the hydride-transfer reactions from BNAH to Q in MeCN as shown in Figure 5.

Although the log *k* values in the presence of Mg^{2+} ion are

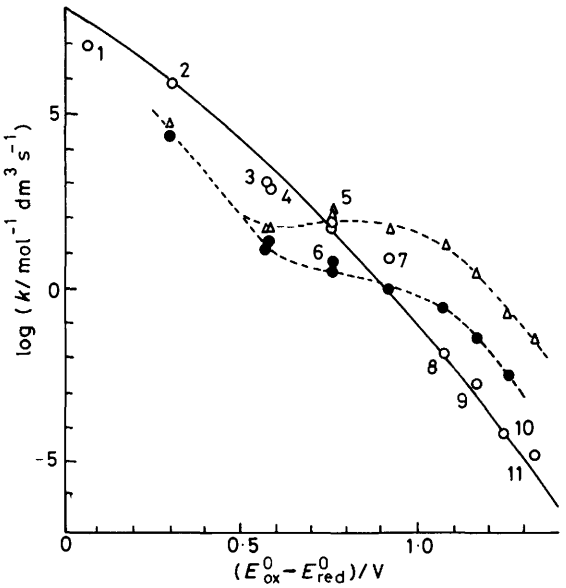

Figure 5. Plots of log *k* for the hydride-transfer reactions from BNAH to *p*-benzoquinone derivatives in the absence (○) and presence of 0.10 mol dm^{-3} (●) and 1.6 mol dm^{-3} (△) Mg^{2+} ion *versus* the difference of the redox potentials between BNAH and *p*-benzoquinone derivatives in the absence of Mg^{2+} ion, $E_{ox}^0 - E_{red}^0$. Numbers refer to *p*-benzoquinone derivatives in Table 1

plotted against the $\Delta G_{et}^0/F$ values in the absence of Mg^{2+} ion in Figure 5, the values of the standard Gibbs energy change of electron transfer from BNAH to Q in the presence of Mg^{2+} ion may be different from those in the absence of Mg^{2+} ion. Indeed, the redox potentials of the reactants (BNAH and Q) in the presence of Mg^{2+} ion vary depending on both the reactants and the Mg^{2+} concentration as shown in Table 3. Thus, the log *k* values in the presence of Mg^{2+} ion in Figure 5 were replotted against the difference between the redox potentials of BNAH and Q in the presence of Mg^{2+} ion, $E_{ox}^{0*} - E_{red}^{0*}$ which has been determined independently based on the analyses of the cyclic voltammograms of BNAH and Q in the presence of Mg^{2+} ion, as shown in Figure 6, where three different correlations between log *k* and $E_{ox}^0 - E_{red}^0$ ($= \Delta G_{et}^0/F$) in Figure 5 emerge as a single and unified one. Such a remarkable transformation of the plots in Figure 5 to the single and unified correlation in Figure 6 underscores the fact that the accelerating and retarding effects of Mg^{2+} ion on the rate constants of hydride-transfer reactions from BNAH to Q are well reflected in the change of the redox potentials of BNAH and Q in the presence of Mg^{2+} ion.

Simulation of Correlation between log k and $\Delta G_{et}^{0*}/F$ *by the Marcus Formalism.*—The single and unified correlation between log *k* and $E_{ox}^{0*} - E_{red}^{0*}$ ($= \Delta G_{et}^{0*}/F$) in Figure 6 can be evaluated quantitatively based on the reaction mechanism [equations (1) and (2)] as follows. According to equations (1) and (2), the rate constant for the hydride transfer from BNAH to Q is given by equation (15), where K_{et} ($= K_{CT}k_1/k_{-1}$)

$$k = k_H K_{et} \quad (15)$$

corresponds to the formation constant of the radical ion pair [$BNAH^{+\bullet}$ $Q^{-\bullet}$] and the rate constant for the electron transfer from $BNA^{\bullet}$ to $QH^{\bullet}$ following the proton transfer from $BNAH^{+\bullet}$ to $Q^{-\bullet}$ is not included since the electron transfer, being highly exothermic [the redox potentials of $BNA^{\bullet}$ (−1.2 V *versus* s.c.e.)[28] is much more negative than the redox potentials of

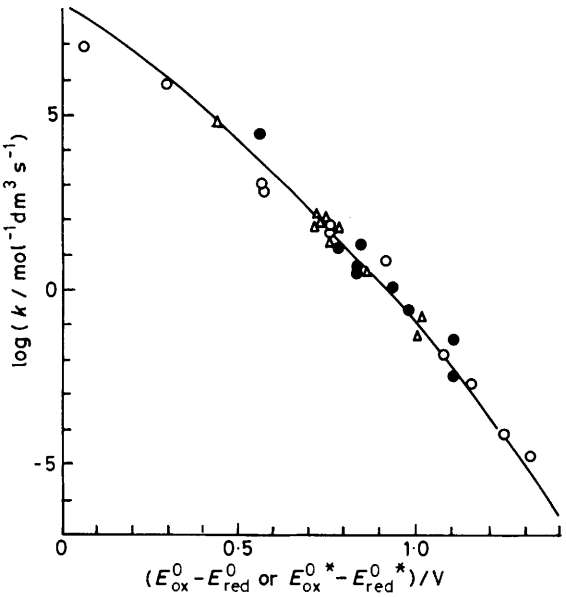

Figure 6. Plot of log k for the hydride-transfer reactions from BNAH to *p*-benzoquinone derivatives in the absence (○) and presence of 0.10 mol dm^{-3} (●) and 1.6 mol dm^{-3} (△) Mg^{2+} ion *versus* the difference between the redox potentials of BNAH and *p*-benzoquinone derivatives in the absence and presence of 0.10 and 1.6 mol dm^{-3} Mg^{2+} ion, respectively

$QH^{\bullet}$[29]], may be very rapid. Thus, the rate constant for the hydride transfer k can be divided into two components, *i.e.* the rate constant for the proton transfer k_H and the formation constant of the radical ion pair K_{et}, both of which can be evaluated quantitatively as a function of the standard Gibbs energy change of the electron transfer from BNAH to Q, $\Delta G_{et}^0 = F(E_{ox}^0 - E_{red}^0)$.

First, the log K_{et} value is related directly to the Gibbs energy change for the formation of the radical ion pair ΔG_{et} (BNAH + Q ⟶ [$BNAH^{+\bullet}$ $Q^{-\bullet}$]) by equation (16). The ΔG_{et} value may

$$\log K_{et} = -\Delta G_{et}/2.3RT \quad (16)$$

be obtained by equation (17), where the standard Gibbs energy

$$\Delta G_{et} = \Delta G_{et}^0 + w_p \quad (17)$$

change of the electron transfer (BNAH + Q ⟶ $BNAH^{+\bullet}$ + $Q^{-\bullet}$) ΔG_{et}^0 is obtained from equation (14) and the work term w_p required to bring the products ($BNAH^{+\bullet}$ and $Q^{-\bullet}$) to their mean separation in the activated complex may be constant for a series of *p*-benzoquinone derivatives. Then, by combining equations (16) and (17), log K_{et} is given as a linear function of ΔG_{et}^0 with a slope of $-1/2.3RT$ which corresponds to -16.9 at 298 K [equation (18), where C_1 is a constant ($-w_p/2.3RT$)].

$$\log K_{et} = -\Delta G_{et}^0/2.3RT + C_1 \quad (18)$$

Since the log K_{et} value in the case of 2,3-dichloro-5,6-dicyano-*p*-benzoquinone has previously been reported as 4.3,[12] and the $\Delta G_{et}^0/F$ value is obtained from the redox potentials of BNAH and 2,3-dichloro-5,6-dicyano-*p*-benzoquinone in the absence of Mg^{2+} ion in Table 3 (E_{ox}^0 0.57 and E_{red}^0 0.51 V, respectively), the C_1 value in equation (18) is determined as 5.3.

On the other hand, the activation Gibbs energy for the proton transfer from $BNAH^{+\bullet}$ to $Q^{-\bullet}$, $\Delta G_H^{\ddagger}$, can be expressed as a function of the Gibbs energy change of the proton transfer ΔG ($= -2.3RT\Delta pK_a$) by using the Marcus formalism [equations (19)—(21),[11,30] where $\Delta G_{H0}^{\ddagger}$ is the intrinsic barrier for the

$$\Delta G_H^{\ddagger} = \Delta G_{H0}^{\ddagger}[1 + (\Delta G/4\Delta G_{H0}^{\ddagger})]^2 \quad \text{when } -4\Delta G_{H0}^{\ddagger} < \Delta G < 4\Delta G_{H0}^{\ddagger} \quad (19)$$

$$\Delta G_H^{\ddagger} = 0 \quad \text{when } \Delta G < -4\Delta G_{H0}^{\ddagger} \quad (20)$$

$$\Delta G_H^{\ddagger} = \Delta G \quad \text{when } \Delta G > 4\Delta G_{H0}^{\ddagger} \quad (21)$$

proton transfer which corresponds to the activation Gibbs energy when $\Delta pK_a = 0$]. Since there is a linear correlation between pK_a of semiquinone radicals $QH^{\bullet}$ and E_{red}^0 of the corresponding quinones Q,[12,31] ΔG ($= -2.3RT\Delta pK_a$) may be linearly related to ΔG_{et}^0 [$= F(E_{ox}^0 - E_{red}^0)$] as shown by equation (22), where the constant C_2 can be determined,

$$\Delta G = -\alpha\Delta G_{et}^0 + C_2 \quad (22)$$

provided that the α value is given since the pK_a values of $BNAH^{+\bullet}$ and semiquinone radical $QH^{\bullet}$ are known as 3.6[32] and 4.1,[31] respectively, and the redox potentials of BNAH and *p*-benzoquinone Q are given in Table 3. Thus, the proton-transfer rate constant k_H [$=(\kappa T/h)\exp(-\Delta G_H^{\ddagger}/RT)$] can be evaluated as a function of ΔG_{et}^0 by using equations (19)—(22) if the $\Delta G_{H0}^{\ddagger}$ and α values are given.

Taken altogether, the rate constants k for the hydride transfer from BNAH to Q have been calculated from equations (15) and (18)—(22) as a function of $E_{ox}^0 - E_{red}^0$ ($=\Delta G_{et}^0/F$) in the absence of Mg^{2+} ion or $E_{ox}^{0*} - E_{red}^{0*}$ ($=\Delta G_{et}^{0*}/F$) in the presence of Mg^{2+} ion, the values of which are given in Table 3, by using the values of $\Delta G_{H0}^{\ddagger}$ = 12.6 kJ mol^{-1} and α = 0.58 as the best-fit parameters. The results are shown as the solid line in Figure 6, where the calculated line agrees well with the experimental plot. Although the choice of the parameters $\Delta G_{H0}^{\ddagger}$ and α is somehow arbitrary, the $\Delta G_{H0}^{\ddagger}$ value used in this study (12.6 kJ mol^{-1}) is typical as the intrinsic barrier of proton-transfer reactions found in the literature ($\Delta G_{H0}^{\ddagger}$ 12.6 kJ mol^{-1})[33] and the α value (0.58) shows a reasonable agreement with that found as the slope (0.50) in the plot of pK_a of semiquinone radicals against $-FE_{red}^0/2.3RT$ of the corresponding quinones.[12]

Effects of Mg^{2+} *Ion on Primary Kinetic Isotope Effects* k_H/k_D *for Hydride Transfer from BNAH to Q.*—The primary kinetic isotope effects k_H/k_D for the hydride-transfer reactions from BNAH to Q listed in Table 2 are plotted against the difference between the redox potentials of BNAH and Q in the absence of Mg^{2+} ion, $E_{ox}^0 - E_{red}^0$, as shown in Figure 7, where the upper abscissa indicates the Gibbs energy change of the proton transfer ΔG ($= -2.3RT\Delta pK_a$) which is linearly related to the bottom abscissa $E_{ox}^0 - E_{red}^0$ ($=\Delta G_{et}^0/F$) by equation (22). The k_H/k_D value in the absence of Mg^{2+} ion shows a bell-shaped dependence on the $E_{ox}^0 - E_{red}^0$ value with a maximum value 6.2. Since the rate constant k corresponds to $k_H K_{et}$ [equation (15)] and no primary kinetic isotope effect is expected for the formation of the radical ion pair (K_{et}), the primary kinetic isotope effects k_H/k_D observed for the hydride-transfer reactions from BNAH to Q may be ascribed to those for the proton transfer from $BNAH^{+\bullet}$ to $Q^{-\bullet}$ in the radical ion pair. In such a case, k_H/k_D may be expressed as a function of the Gibbs energy change of the proton transfer ΔG, using the Marcus formalism [equation (19)] where $\Delta G_D^{\ddagger}$ can be calculated by substituting $\Delta G_{H0}^{\ddagger}$ by $\Delta G_{D0}^{\ddagger}$, as shown by equation (23). Thus, it is expected that the log (k_H/k_D) value shows a parabolic dependence on ΔG and the maximum k_H/k_D values are reached when ΔG = 0. It

$$2.3RT\log(k_H/k_D) = \Delta G_{D0}^{\ddagger} - \Delta G_{H0}^{\ddagger} + \frac{(\Delta G)^2}{16}\left(\frac{1}{\Delta G_{D0}^{\ddagger}} - \frac{1}{\Delta G_{H0}^{\ddagger}}\right) \quad (23)$$

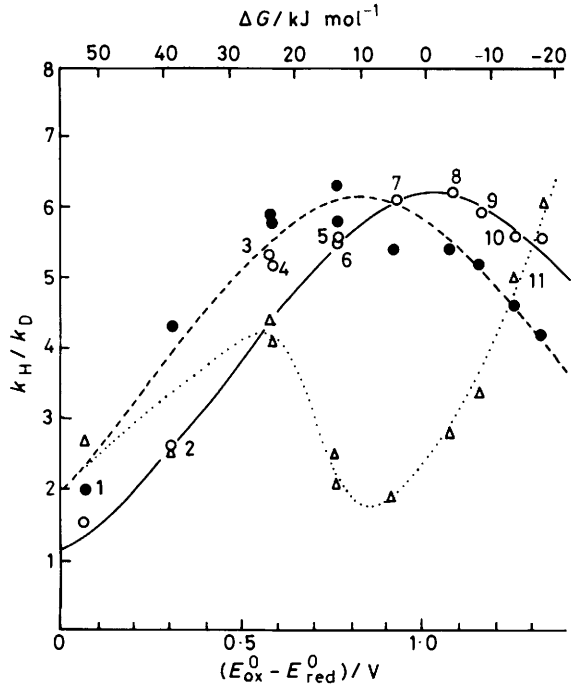

Figure 7. Plots of the primary kinetic isotope effects k_H/k_D for the hydride-transfer reactions from BNAH to *p*-benzoquinone derivatives in the absence (○) and presence of 1.0×10^{-2} mol dm^{-3} (●) and 1.6 mol dm^{-3} (△) Mg^{2+} ion *versus* the difference between the redox potentials of BNAH and *p*-benzoquinone derivatives in the absence of Mg^{2+} ion, $E_{ox}^0 - E_{red}^0$. The ΔG is shown in the upper abscissa, which is related to the bottom abscissa by equation (22). Numbers refer to *p*-benzoquinone derivatives in Table 1

should be emphasized that, indeed, the k_H/k_D value in the absence of Mg^{2+} ion reaches the maximum when $\Delta G = 0$, as shown in Figure 7. Then, the maximum k_H/k_D value (6.2) corresponds to $\exp[(\Delta G_{D0}^{\ddagger} - \Delta G_{H0}^{\ddagger})/RT]$ from equation (23) when $\Delta G = 0$, and thereby the $\Delta G_{D0}^{\ddagger} - \Delta G_{H0}^{\ddagger}$ value is obtained as 4.5 kJ mol^{-1}. By using the $\Delta G_{D0}^{\ddagger} - \Delta G_{H0}^{\ddagger}$ value, the dependence of k_H/k_D in the absence of Mg^{2+} ion on ΔG is calculated by using equation (23) as shown by the solid line in Figure 7, which agrees well with the experimental plot. Such an agreement demonstrates the validity of the present analyses on log k and k_H/k_D based on the reaction mechanism [equations (1) and (2)].

The plot of k_H/k_D in the presence of 1.0×10^{-2} mol dm^{-3} Mg^{2+} ion *versus* $E_{ox}^0 - E_{red}^0$ shows approximately a parallel shift in the negative direction (−0.2 V) relative to that in the absence of Mg^{2+} ion (Figure 7). Such a parallel shift (−0.2 V) may be explained by the formation of a ternary complex [BNAH Mg^{2+} Q] [equation (7)] where the Mg^{2+} ion may interact only with BNAH in the low Mg^{2+} concentration (1.0×10^{-2} mol dm^{-3}), since the separate plots of k_H/k_D in the absence and presence of 1.0×10^{-2} mol dm^{-3} Mg^{2+} ion (Figure 7) may emerge as a single and unified plot if the E_{ox}^{0*} value of BNAH in the presence of Mg^{2+} ion, which is shifted by *ca.* 0.2 V relative to that in the absence of Mg^{2+} ion (Table 3), would be used in the bottom abscissa $E_{ox}^0 - E_{red}^0$. Indeed, the CT band of the ternary complex in the case of 2,6-dichloro-*p*-benzoquinone (Figure 2) also is blue-shifted by 0.25 eV relative to that in the absence of Mg^{2+} ion, which is compatible with the positive shift of the E_{ox}^{0*} value of BNAH in the presence of Mg^{2+} ion.

The plot of k_H/k_D in the presence of much more concentrated Mg^{2+} ion (1.6 mol dm^{-3}) *versus* $E_{ox}^0 - E_{red}^0$ is close to those in the absence and presence of 1.0×10^{-2} mol dm^{-3} Mg^{2+} ion for *p*-benzoquinone derivatives (nos. 1—4) with reduction potentials which are approximately invariant in the presence of 1.6 mol dm^{-3} Mg^{2+} ion (Table 3), but is significantly shifted in the positive direction for *p*-benzoquinone derivatives (nos. 5—11) with reduction potentials which show positive shifts in the presence of 1.6 mol dm^{-3} Mg^{2+} ion (Table 3).

Thus, the change of the primary kinetic isotope effects k_H/k_D in the presence of Mg^{2+} ion is also consistent with that of the redox potentials of BNAH and Q although no quantitative analysis for the effects of Mg^{2+} ion on k_H/k_D has been performed.

References

1 R. H. Abeles, R. F. Hutton, and F. H. Westheimer, *J. Am. Chem. Soc.*, 1957, **79**, 712; D. C. Dittmer and R. A. Fouty, *ibid.*, 1964, **86**, 91; C.-H. Wang, S. M. Linnel, and N. Wang, *J. Org. Chem.*, 1971, **36**, 525.

2 J. W. Bunting and S. Sindhuatmadja, *J. Org. Chem.*, 1981, **46**, 4211; J. W. Bunting, V. S. F. Chew, and G. Chu, *ibid.*, 1982, **47**, 2303.

3 R. Stewart and D. J. Norris, *J. Chem. Soc., Perkin Trans. 2*, 1978, 246; R. Srinivasan, R. T. Medary, H. F. Fisher, D. J. Norris, and R. Stewart, *J. Am. Chem. Soc.*, 1982, **104**, 807.

4 M. F. Powell and T. C. Bruice, *J. Am. Chem. Soc.*, 1983, **105**, 1014, 7139; D. M. Chipman, R. Yaniv, and P. van Eikeren, *ibid.*, 1980, **102**, 3244; A. van Laar, H. J. van Ramesdonk, and J. W. Verhoeven, *Recl. Trav. Chim. Pays-Bas*, 1983, **102**, 157.

5 S.-K. Chung and S.-U. Park, *J. Org. Chem.*, 1982, **47**, 3197; I. MacInnes, D. C. Nonhebel, S. T. Orszulik, and C. J. Suckling, *J. Chem. Soc., Perkin Trans. 1*, 1983, 2777; J. C. G. van Nield and U. K. Pandit, *J. Chem. Soc., Chem. Commun.*, 1983, 149.

6 J. J. Steffens and D. M. Chipman, *J. Am. Chem. Soc.*, 1971, **93**, 6694; D. J. Creighton, J. Hajdu, G. Mooser, and D. S. Sigman, *ibid.*, 1973, **95**, 6855; D. S. Sigman, J. Hajdu, and D. J. Creighton, 'Bioorganic Chemistry,' ed. E. E. van Tamelen, Academic Press, New York, 1978, vol. IV, p. 385.

7 A. Ohno, T. Shio, H. Yamamoto, and S. Oka, *J. Am. Chem. Soc.*, 1981, **103**, 2045; A. Ohno, J. Nakai, K. Nakamura, T. Goto, and S. Oka, *Bull. Chem. Soc. Jpn.*, 1981, **54**, 3486; A. Ohno, H. Kobayashi, S. Oka, and T. Goto, *Tetrahedron Lett.*, 1983, **24**. 5123; A. Ohno, H. Kobayashi, K. Nakamura, and S. Oka, *ibid.*, p. 1263.

8 S. Shinkai, T. Tsuno, Y. Asatani, and O. Manabe, *J. Chem. Soc., Perkin Trans. 2*, 1983, 1533; S. Yasui, K. Nakamura, A. Ohno, and S. Oka, *Bull. Chem. Soc. Jpn.*, 1982, **55**, 196; S. Yasui, K. Nakamura, and A. Ohno, *Tetrahedron Lett.*, 1983, **24**, 3331; S. Fukuzumi, Y. Kondo, and T. Tanaka, *Chem. Lett.*, 1983, 751.

9 C. C. Lai and A. K. Colter, *J. Chem. Soc., Chem. Commun.*, 1980, 1115; W. F. Jarvis and D. C. Dittmer, *J. Org. Chem.*, 1983, **48**, 2784.

10 R. M. G. Roberts, D. Ostovic, and M. M. Kreevoy, *Faraday Discuss. Chem. Soc.*, 1982, **74**, 257; D. Ostovic, R. M. G. Roberts, and M. M. Kreevoy, *J. Am. Chem. Soc.*, 1983, **105**, 7629.

11 R. A. Marcus, *J. Phys. Chem.*, 1968, **72**, 891.

12 S. Fukuzumi, N. Nishizawa, and T. Tanaka, *J. Org. Chem.*, 1984, **49**, 3571; S. Fukuzumi and T. Tanaka, *Chem. Lett.*, 1982, 1513.

13 D. J. Creighton and D. S. Sigman, *J. Am. Chem. Soc.*, 1971, **93**, 6314; D. J. Creighton. J. Hajdu, and D. S. Sigman, *ibid.*, 1976, **98**, 4619; S. Shinkai and T. C. Bruice, *ibid.*, 1972, **94**, 8258; M. Shirai, T. Chishina, and M. Tanaka, *Bull. Chem. Soc. Jpn.*, 1975, **48**, 1079; Y. Ohnishi, M. Kagami, and A. Ohno, *J. Am. Chem. Soc.*, 1975, **97**, 4766; M. Hughes and R. H. Prince, *Chem. Ind. (London)*, 1975, 648; K. Watanabe, R. Kawaguchi, and H. Kato, *Chem. Lett.*, 1978, 255; Y. Murakami, Y. Aoyama, and J. Kikuchi, *Bull. Chem. Soc. Jpn.*, 1982, **55**, 2898.

14 Y. Ohnishi, M. Kagami, and A. Ohno, *Tetrahedron Lett.*, 1975, 2437; Y. Ohnishi and M. Kitami, *ibid.*, 1978, 4033; Y. Ohnishi, T. Numakunai, T. Kimura, and A. Ohno, *ibid.*, 1976, 2699; A. Ohno, H. Yamamoto, and S. Oka, *J. Am. Chem. Soc.*, 1981, **103**, 2041.

15 R. A. Gase and U. K. Pandit, *J. Am. Chem. Soc.*, 1979, **101**, 7059; M. Hughes and R. H. Prince, *J. Inorg. Nucl. Chem.*, 1978, **40**, 703; R. A. Gase, G. Boxhoorn, and U. K. Pandit, *Tetrahedron Lett.*, 1976, 2889.

16 S. Shinkai, T. Ide, H. Hamada, O. Manabe, and T. Kunitake, *J. Chem. Soc., Chem. Commun.*, 1977, 848; A. Ohno, S. Yasui, K. Nakamura, and S. Oka, *Bull. Chem. Soc. Jpn.*, 1978, **51**, 290; A. Ohno, S. Yasui, H. Yamamoto, S. Oka, and Y. Ohnishi, *ibid.*, p. 294; A. Ohno, H. Yamamoto, and S. Oka, *Tetrahedron Lett.*, 1979, 4061.

17 S. Fukuzumi, Y. Kondo, and T. Tanaka, *Chem. Lett.*, 1983, 485.
18 A preliminary report has appeared, S. Fukuzumi, N. Nishizawa, and T. Tanaka, *Chem. Lett.*, 1983, 1755.
19 A. G. Anderson, Jr., and G. Berkelhammer, *J. Am. Chem. Soc.*, 1958, **80**, 992; D. Mauzerall and F. H. Westheimer, *ibid.*, 1955, **77**, 2261.
20 W. S. Caughey and K. A. Schellenberg, *J. Org. Chem.*, 1966, **31**, 1978.
21 D. D. Perrin, W. L. Armarego, and D. R. Perrin, 'Purification of Laboratory Chemicals,' Pergamon Press, New York, 1966.
22 J. Cason, C. F. Allen, and S. Goodwin, *J. Org. Chem.*, 1948, **13**, 403; A. G. Brook, *J. Chem. Soc.*, 1953, 5040.
23 Y. Matsunaga, *J. Chem. Phys.*, 1964, **41**, 1609.
24 S. Fukuzumi, K. Hironaka, N. Nishizawa, and T. Tanaka, *Bull. Chem. Soc. Jpn.*, 1983, **56**, 2220.
25 R. J. Klingler, S. Fukuzumi, and J. K. Kochi, *Am. Chem. Soc. Symp. Ser.*, 1983, **211**, 117; R. J. Klingler and J. K. Kochi, *J. Am. Chem. Soc.*, 1980, **102**, 4790; 1981, **103**, 5839; 1982, **104**, 4186; *J. Phys. Chem.*, 1981, **85**, 1731.
26 D. H. Evans, 'Encyclopedia of Electrochemistry of the Elements, Organic Section,' ed. A. J. Bard and H. Lund, Marcel Dekker, New York, 1978, ch. XII-1, and references therein; Y. Iida and H. Akamatsu, *Bull. Chem. Soc. Jpn.*, 1967, **40**, 231.
27 R. A. Marcus, *J. Phys. Chem.*, 1963, **67**, 853; *Annu. Rev. Phys. Chem.*, 1964, **15**, 155.
28 R. F. Anderson, *Biochim. Biophys. Acta*, 1980, **590**, 277; J. A. Farrington, E. J. Land, and A. J. Swallow, *ibid.*, p. 273; A. J. Cunningham and A. L. Underwood, *Biochemistry*, 1967, **6**, 266; J. Hermolin, E. K. Eisner, and E. M. Kosower, *J. Am. Chem. Soc.*, 1981, **103**, 1591.
29 G. Dryhurst, K. M. Kadish, F. Scheller, and R. Renneberg, 'Biological Electrochemistry,' Academic Press, New York, 1982, and references therein.
30 A. J. Kresge, *Chem. Soc. Rev.*, 1973, **2**, 475.
31 K. B. Patel and R. L. Willson, *J. Chem. Soc., Faraday Trans. 1*, 1973, **69**, 814.
32 S. Fukuzumi, Y. Kondo, and T. Tanaka, *J. Chem. Soc., Perkin Trans. 2*, 1984, 673.
33 R. P. Bell, 'The Proton in Chemistry,' Cornell University Press, Ithaca, 1959, p. 172; M. M. Kreevoy and S.-W. Oh, *J. Am. Chem. Soc.*, 1973, **95**, 4805; W. J. Albery, A. N. Campbell-Crawford, and J. S. Curran, *J. Chem. Soc., Perkin Trans. 2*, 1972, 2206; M. L. Ahrens, M. Eigen, W. Kruse, and G. Maass, *Ber., Bunsenges. Phys. Chem.*, 1970, **74**, 380.

Received 2nd April 1984; *Paper* 4/535